

## Characterization of Silica-Supported Molybdenum Oxide and Tungsten Oxide. Reducibility of the Oxidic State versus Hydrodesulfurization Activity of the Sulfided State<sup>1</sup>

R. THOMAS,<sup>2</sup> E. M. VAN OERS,\* V. H. J. DE BEER,\* AND J. A. MOULIJN†,<sup>3</sup>

†*Institute for Chemical Technology, University of Amsterdam, Plantage Muidergracht 30, 1018 TV, Amsterdam, and \*Eindhoven University of Technology, Laboratory for Inorganic Chemistry and Catalysis, P.O. Box 513, 5600 MB Eindhoven, The Netherlands*

Received July 26, 1982; revised June 9, 1983

Thiophene hydrodesulfurization and butene hydrogenation have been studied for presulfided  $\text{MoO}_3/\text{SiO}_2$  and  $\text{WO}_3/\text{SiO}_2$  catalysts using a micro-flow reactor operating at atmospheric pressure. The catalysts have been prepared by dry as well as wet impregnation. The oxidic precursor catalysts were characterized by X-ray diffraction, surface area and pore volume measurements, and temperature-programmed reduction. Catalysts prepared by dry or wet impregnation are essentially the same. At low metal oxide contents the catalysts are of the monolayer type. At higher metal oxide contents also bulk compounds are present, which is demonstrated by means of X-ray diffraction as well as temperature-programmed reduction. The maximum concentration of monolayer-type compounds corresponds to approximately one transition metal atom per square nanometer of the carrier. A correlation could be established between reducibility of the oxidic monolayer-type catalysts and the activity for thiophene hydrodesulfurization. This correlation appears to be in good agreement with the one reported earlier for the analogous  $\gamma$ -alumina-based catalysts. Butene hydrogenation activity of the sulfided  $\text{MoO}_3/\text{SiO}_2$  and  $\text{WO}_3/\text{SiO}_2$  monolayer-type catalysts also correlates with reducibility of the oxidic systems. Due to the presence of bulk compounds the turnover frequency in hydrodesulfurization as well as hydrogenation decreases at higher metal oxide contents.

### INTRODUCTION

In a previous paper (1) a relation was demonstrated to exist between the reducibility of oxidic  $\text{MoO}_3/\gamma\text{-Al}_2\text{O}_3$  and  $\text{WO}_3/\gamma\text{-Al}_2\text{O}_3$  monolayer catalyst systems and the thiophene hydrodesulfurization (HDS) as well as butene hydrogenation activity of these catalysts in their sulfided form. It was concluded that temperature-programmed reduction (TPR) analysis can be applied as a time-saving preliminary screening technique in the development of monolayer type oxidic precursors for HDS catalysts.

<sup>1</sup> This study is part of the Ph.D. thesis of R. Thomas, University of Amsterdam, 1981.

<sup>2</sup> Present address: Institute for Environmental Studies, Free University, P.O. Box 7161, 1007 MC Amsterdam, The Netherlands.

<sup>3</sup> Author to whom correspondence should be addressed.

At low transition metal contents both the catalytic activity per mol Mo or W and the reducibility were found to be low. These two effects were attributed to a strong interaction between the alumina carrier and the transition metal compound.

From a practical point of view it is useful to investigate whether the efficiency (activity per mol active phase) can be increased, for example by applying a less reactive carrier material such as silica which interacts weakly with the active phase. Such a weak interaction, however, easily leads to a lower dispersion of the active phase, which can become manifest by the formation of crystalline material. Therefore, in order to determine whether TPR can be applied as a screening technique for catalysts which are not of the monolayer type, it is necessary to know the effect of bulk compounds on re-

ducibility and HDS activity. It is reasonable to expect that reduction kinetics for bulk compounds are different from kinetics of highly dispersed surface compounds. In the case of bulk compounds the reduction process can be described by the shrinking core model (2), often showing nucleation characteristics. This means that the reduction rate is determined at first by the formation of nuclei at the surface of the support particles. For reduction of a monolayer, nucleation is often not important and the reduction rate will depend mainly on the variation in chemical properties of the surface species, such as interaction with the support and degree of aggregation. Thus, a priori, differences can be anticipated in the nature of the various TPR patterns, viz. reduction temperature and shape of the TPR band.

Obviously it is important to know the fraction of transition metal atoms present as surface or bulk compounds. The amount of crystalline bulk compounds can be determined by various methods such as X-ray diffraction (XRD), x-ray photoelectron spectroscopy (XPS), Raman spectroscopy, and temperature-programmed reduction (3–7). For the  $\text{MoO}_3/\text{SiO}_2$  and  $\text{WO}_3/\text{SiO}_2$  catalysts studied here, XPS and XRD were found to give consistent results (4).

In order to be able to compare these series of catalysts properly with alumina-supported systems described previously (1), the range of calculated surface coverage (transition metal atoms/ $\text{nm}^2$  carrier surface) was kept the same for the silica- and alumina-supported catalysts. It should be noted that for the silica-based systems the calculated surface coverage is not necessarily the same as the actual surface coverage, since at higher metal contents crystalline material is also present.

#### METHODS

**Catalyst preparation.** Catalysts were prepared by impregnation of a Grace silica (type 62, pore volume  $1.1 \text{ cm}^3 \text{ g}^{-1}$ , surface area  $360 \text{ m}^2 \text{ g}^{-1}$ , particle size  $180\text{--}210 \mu\text{m}$ )

with aqueous solutions of ammonium heptamolybdate (Merck, min 99%) or ammonium metatungstate (Koch-Light, min 99.9%). Wet and dry impregnation was carried out using 5.5 and  $1.1 \text{ cm}^3$  solution per gram of carrier, respectively. The impregnated samples were dried at 393 K (16 h) and calcined under fluidizing conditions at 823 K in dry air (2 h).

**X-Ray diffraction.** The XRD patterns were recorded on a Philips PW 1050-25 vertical diffractometer.

**Specific surface area and pore volume measurements.** The specific surface area and pore volume of the catalysts were determined according to the BET method on a Carlo Erba Sorptomatic instrument (nitrogen adsorption at 79 K; area of  $\text{N}_2$  molecule  $0.1627 \text{ nm}^2$ ). Pore volumes were also measured via water titration. The surface areas and pore volumes per gram of carrier were calculated from the experimental values for the catalysts and the metal oxide contents.

**Transition metal content determination.** Mo and W content of the samples were analyzed by means of a Perkin-Elmer 300 atomic absorption spectrometer (AAS), by X-ray fluorescence (XRF) using a Philips 1410 X-ray spectrometer, and by means of TPR.

**Temperature-programmed reduction.** The size of the samples was varied with the Mo(W) content in such a way that each sample contained approximately 0.2 mmol of transition metal ions. Samples were reduced in a stream of hydrogen/nitrogen or a hydrogen/argon mixture (flow rate  $12.5 \mu\text{mol s}^{-1}$ ) from 473 to 1333 K at a constant heating rate of  $5 \text{ K min}^{-1}$  in a quartz tube (inner diameter 4.5 mm).

Reduction leads to a decrease in hydrogen concentration, which was detected by a thermal conductivity cell. Each sample was preheated *in situ* in air (773 K, 1 h) in order to be sure that all Mo and W species were fully oxidized, and subsequently cooled under vacuum to 473 K.

The  $\text{H}_2/\text{N}_2$  mixture (Hoek Loos, 99.9%,  $\text{H}_2$  mol fraction 0.67) and  $\text{H}_2/\text{Ar}$  mixture

(Matheson, RP, H<sub>2</sub> mol fraction: 0.69) were purified over a deoxygenation catalyst (BASF, R311) and molecular sieves (Merck 3A).

**Activity measurements.** Hydrodesulfurization experiments were carried out in a stainless-steel microflow reactor device operating at atmospheric pressure and fitted with a quartz reactor tube (inner diameter 8 mm). A detailed description has been published previously (8).

Prior to the activity test the samples (normally 0.5 g) were presulfided *in situ* in a mixture of hydrogen (Hoek Loos 99.9%) and hydrogen sulfide (Matheson C.P.) at atmospheric pressure. The H<sub>2</sub>S concentration was 10 mol% and the total flow rate 42  $\mu\text{mol s}^{-1}$ . The temperature was increased to 673 K according to the following program: 10 min at 295 K, linear temperature increase to 673 K in 1 h, isothermal at 673 K for 2 h. After the sulfiding procedure a mixture of hydrogen (Hoek Loos 99.9%) and thiophene (Merck, min 99%), mol fraction thiophene 6.2 mol%, was fed to the reactor at a flow rate of 35  $\mu\text{mol s}^{-1}$ . Reaction products were analyzed by gas chromatography. HDS activity and butene hydrogenation activity were calculated from analysis data obtained after a run of 2 h.

**X-Ray photoelectron spectroscopy.** The XPS spectra were recorded on a AEI ES-200 spectrometer, using an AlK $\alpha$  source (1496 eV) with a linewidth of 0.7 eV. The spectrometer was evacuated to better than 13  $\mu\text{Pa}$  ( $10^{-7}$  Torr), and the data were collected on a PDP-8 computer. The source power was 180 mW and the temperature of the samples was kept at approximately 283 K. The powdered samples were mounted on double-sided adhesive tape.

## RESULTS

### Textural Properties

Surface areas and pore volumes are given in Table 1. It is clear that the preparation method, viz. dry or wet impregnation, is not critical, because only minor differences

are observed. Also pore radius distributions, not given in Table 1, are not sensitive to the preparation method applied.

For WO<sub>3</sub>/SiO<sub>2</sub> the surface area per gram carrier is approximately constant; for MoO<sub>3</sub>/SiO<sub>2</sub> a decrease is observed at increasing Mo content. The same effect has been observed by Kerkhof *et al.* (9) for WO<sub>3</sub>/SiO<sub>2</sub> and by Castellan *et al.* (10) for MoO<sub>3</sub>/SiO<sub>2</sub>. For both MoO<sub>3</sub>/SiO<sub>2</sub> and WO<sub>3</sub>/SiO<sub>2</sub> the pore volumes calculated per gram carrier are essentially the same.

### Transition Metal Content

Catalyst composition expressed as weight percentage MoO<sub>3</sub>(WO<sub>3</sub>) and Mo(W) atom/nm<sup>2</sup> (see Table 1) are obtained by averaging the results of XRD, AAS, and TPR analysis, which were found to agree within 10%.

### X-Ray Diffraction and X-Ray Photoelectron Spectroscopy

In the XRD patterns, lines of crystalline MoO<sub>3</sub> and WO<sub>3</sub> are present at calculated surface coverages above ca. 1 transition metal atom/nm<sup>2</sup>. However, the relative intensities of the MoO<sub>3</sub> lines deviate from those reported by the JCPDS card (11); particularly the intensity of the line at  $2\theta = 25.7^\circ$  is too low. From line broadening (3) it was derived that the crystal diameters are approximately 30 and 20 nm for MoO<sub>3</sub>/SiO<sub>2</sub> and WO<sub>3</sub>/SiO<sub>2</sub>, respectively. For both series the crystallite sizes are independent of the transition metal content. From XRD and XPS intensities the amount of crystalline material was determined (4). Table 2 gives the combined results. The concentration of transition metal atoms present as noncrystalline material is limited to approximately 1 atom/nm<sup>2</sup>.

### Temperature-Programmed Reduction

The TPR patterns reported here were recorded using a H<sub>2</sub>/N<sub>2</sub> mixture. Only the pattern of MoO<sub>3</sub> was determined using a H<sub>2</sub>/Ar mixture. The reason was that during the reduction of MoO<sub>3</sub> in H<sub>2</sub>/N<sub>2</sub> mixture nitride

TABLE 1  
Composition, Surface Area, Pore Volume, Thiophene Hydrodesulfurization, Activity Data, and Average Reduction Temperature of the Catalysts

Catalysts	Metal oxide content		BET area (m <sup>2</sup> g <sup>-1</sup> )		Pore volume (cm <sup>3</sup> g <sup>-1</sup> )			Product gas composition (mol%)			$k_1$ m <sup>3</sup> Thiophene converted (mol metal) <sup>-1</sup> s <sup>-1</sup> × 10 <sup>-3</sup>	$k_2$ m <sup>3</sup> Butene converted (mol metal) <sup>-1</sup> s <sup>-1</sup> × 10 <sup>-3</sup>	$T_{red}$ (K)
	(atom/nm <sup>2</sup> )	(wt%)	a	b	a	b		Thiophene	Butenes	Butanes			
MoO <sub>3</sub> /SiO <sub>2</sub> dry impregnation	0.11	0.9	340	345	0.95	0.96		98.7	1.3	b.d.l.	0.80	—	790
	0.21	1.8	340	345	0.95	0.97		97.3	2.7	b.d.l.	0.84	—	790
	0.40	3.3	310	320	0.95	0.98		92.3	7.2	0.5	1.34	2.01	800
	0.89	7.1	280	300	0.92	0.99		79.7	17.2	3.1	1.76	2.55	790
	1.54	11.7	230	260	0.85	0.96		76.1	19.1	4.8	1.29	2.09	760
	4.14	26.3	185	250	0.61	0.83		73.4	20.5	6.1	0.65	1.09	790
MoO <sub>3</sub> /SiO <sub>2</sub> wet impregnation	0.09	0.8	370	375	1.01	1.02		—	—	—	—	—	750
	0.20	1.7	355	360	0.97	0.99		—	—	—	—	—	750
	0.33	2.8	350	360	0.98	1.01		93.2	6.4	0.4	1.39	2.31	770
	0.79	6.4	315	335	0.91	0.97		84.2	13.9	1.9	1.48	2.21	800
	1.69	12.7	255	290	0.86	0.99		76.7	18.9	4.4	1.15	1.81	780
	3.16	21.4	195	250	0.74	0.94		74.2	19.9	5.9	0.77	1.33	750
WO <sub>3</sub> /SiO <sub>2</sub> wet impregnation	0.08	1.1	—	—	0.98	0.99		—	—	—	—	—	1000
	0.21	2.8	360	370	0.97	1.00		98.8	1.2	b.d.l.	0.38	—	990
	0.44	5.7	—	—	0.95	1.01		96.9	3.0	0.1	0.49	—	910
	0.93	11.4	—	—	0.87	0.98		92.0	7.2	0.8	0.65	1.65	910
	1.88	20.7	295	370	0.78	0.98		89.4	9.1	1.5	0.48	1.32	890
	3.98	35.6	220	340	0.61	0.95		83.2	13.6	3.2	0.46	1.07	870
WO <sub>3</sub> /SiO <sub>2</sub> dry impregnation	0.12	1.6	—	—	0.98	1.00		—	—	—	—	—	970
	0.23	3.1	—	—	0.97	1.00		98.8	1.2	b.d.l.	0.35	—	950
	0.44	5.8	—	—	0.92	0.98		96.7	3.1	0.2	0.51	1.61	930
	0.49	6.4	345	370	0.92	0.98		—	—	—	—	—	940
	1.09	13.1	—	—	0.87	1.00		91.6	7.4	1.1	0.60	1.88	910
	4.79	39.9	195	325	0.51	0.85		81.4	14.5	4.0	0.46	1.08	920
MoO <sub>3</sub>	—	99.9	—	13	—	—		96.0	3.7	0.3	0.02	0.09	850
WO <sub>3</sub>	—	99.9	—	17	—	—		93.1	6.1	0.8	0.06	0.22	840

Note. a = calculated per gram catalyst; b = calculated per gram carrier. — = not measured. b.d.l. = below detection limit.

TABLE 2

Fraction of Crystalline  $\text{MoO}_3(\text{WO}_3)$  and Surface Concentration of Noncrystalline Molybdate (Tungstate) Estimated from the Combined Results of X-Ray Photoelectron Spectroscopy and X-Ray Diffraction Analysis

Catalysts	Metal content		Fraction of crystalline $\text{MoO}_3(\text{WO}_3)$	Noncrystalline surface concentration (atom/nm <sup>2</sup> ) <sup>b</sup>
	wt%	atom/nm <sup>2</sup> <sup>a</sup>		
$\text{MoO}_3/\text{SiO}_2$ dry impregnation	7.1	0.89	0.10	0.8
	11.7	1.54	0.25	1.2
	26.3	4.14	0.70	1.2
$\text{MoO}_3/\text{SiO}_2$ wet impregnation	6.4	0.79	0.10	0.7
	12.7	1.69	0.30	1.2
	21.4	3.16	0.60	1.3
$\text{WO}_3/\text{SiO}_2$ dry impregnation	13.1	1.09	0.25	0.8
	39.9	4.79	0.75	1.2
$\text{WO}_3/\text{SiO}_2$ wet impregnation	5.7	0.44	0.05	0.4
	11.4	0.93	0.30	0.7
	20.7	1.88	0.45	1.0
	35.6	3.98	0.75	1.0

<sup>a</sup> Total number of Mo/W atoms divided by the carrier surface area.

<sup>b</sup> Surface concentration of Mo/W atoms present as surface compounds.

formation occurs, thus interfering with the reduction (1). The patterns of  $\text{SiO}_2$ ,  $\text{WO}_3$ , and the catalysts when reduced with  $\text{H}_2/\text{Ar}$  were identical with the patterns obtained with  $\text{H}_2/\text{N}_2$ . For these systems it can be concluded that nitride formation did not interfere.

$\text{MoO}_3/\text{SiO}_2$ . The TPR patterns of  $\text{SiO}_2$ ,  $\text{MoO}_3$ , and  $\text{MoO}_3/\text{SiO}_2$  catalysts prepared by dry and wet impregnation are shown in Fig. 1. Obviously the preparation method is only of minor influence on the shape of the patterns.  $\text{MoO}_3$  reduces at about 900 K. It is clear that the major part of the molybdenum species in the catalysts is reduced at a lower temperature than  $\text{MoO}_3$ . The patterns essentially consist of a peak at about 750 K and a peak at about 900 K. At the lowest contents only the low-temperature peak is observed. Both the intensity of the 900 K peak and the sharpness of the low temperature peak increase with increasing

Mo content. The patterns for the catalysts prepared by wet impregnation show sharper peaks than those of the catalysts prepared by dry impregnation.

From blank experiments ( $\text{SiO}_2$ ) it can be concluded that the support retains a small amount of hydrogen (800–1000 K), which is released at higher temperatures. Since in all measurements a constant amount of transition metal ions is reduced the amount of carrier and consequently the contribution of the silica pattern to the overall pattern of the catalyst decreases at increasing transition metal content.

$\text{WO}_3/\text{SiO}_2$ . The TPR patterns of  $\text{SiO}_2$ ,  $\text{WO}_3$ , and  $\text{WO}_3/\text{SiO}_2$  catalysts prepared by dry and wet impregnation are shown in Fig. 2. Also for these catalysts the preparation method hardly influences the shape of the patterns. In general the tungsten species on the catalysts reduces at higher temperature than  $\text{WO}_3$ , which reduces at approximately

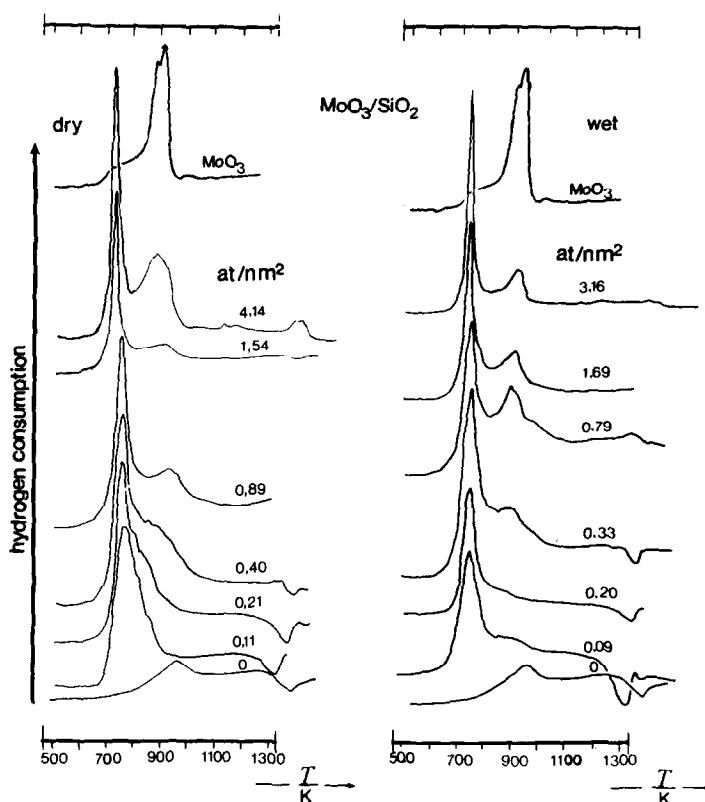


FIG. 1. TPR patterns of  $\text{SiO}_2$ ,  $\text{MoO}_3$ , and  $\text{MoO}_3/\text{SiO}_2$  catalysts prepared by dry and wet impregnation.

800 K. At low W content the TPR patterns of the catalysts consist of several bands, especially for the samples prepared according to the wet impregnation method. At higher W contents the patterns essentially consist of only two bands, viz. one at 800 K and another at 900–950 K.

#### Thiophene Hydrodesulfurization Activity

The activity of the catalysts for thiophene hydrodesulfurization is shown in Fig. 3 as a function of the average Mo(W) surface coverage. For comparison the relation between HDS activity and surface coverage, established for the corresponding  $\text{MoO}_3$ - and  $\text{WO}_3/\gamma\text{-Al}_2\text{O}_3$  samples (1), is also indicated in Fig. 3.

The activity is expressed as the first-order reaction rate constant for hydrodesulfurization divided by the total amount of transition metal atoms in the carrier ( $\text{m}^3$

$\text{mol}^{-1} \text{s}^{-1}$ ) (1). All Mo(W) atoms are thus assumed to be active. No significant differences are observed in catalytic activity of catalysts prepared by dry or wet impregnation. As is also observed for the alumina-supported samples, the Mo-based catalysts are more effective for thiophene HDS than the W-based ones.

For both types of catalyst the HDS activity clearly depends on the surface coverage. It increases up to about 1 Mo(W) atoms/ $\text{nm}^2$ , a value which is far below the theoretical monolayer coverage based on the dimensions of a  $\text{MoO}_3$  unit (12). (It is assumed that the dimensions of a  $\text{WO}_3$  unit are the same.) A gradual decrease is observed at higher coverages, the decrease for  $\text{MoO}_3/\text{SiO}_2$  being much stronger than for  $\text{WO}_3/\text{SiO}_2$ . The results show the same trend as obtained earlier with another set of initially oxidic samples (13). Up to a surface

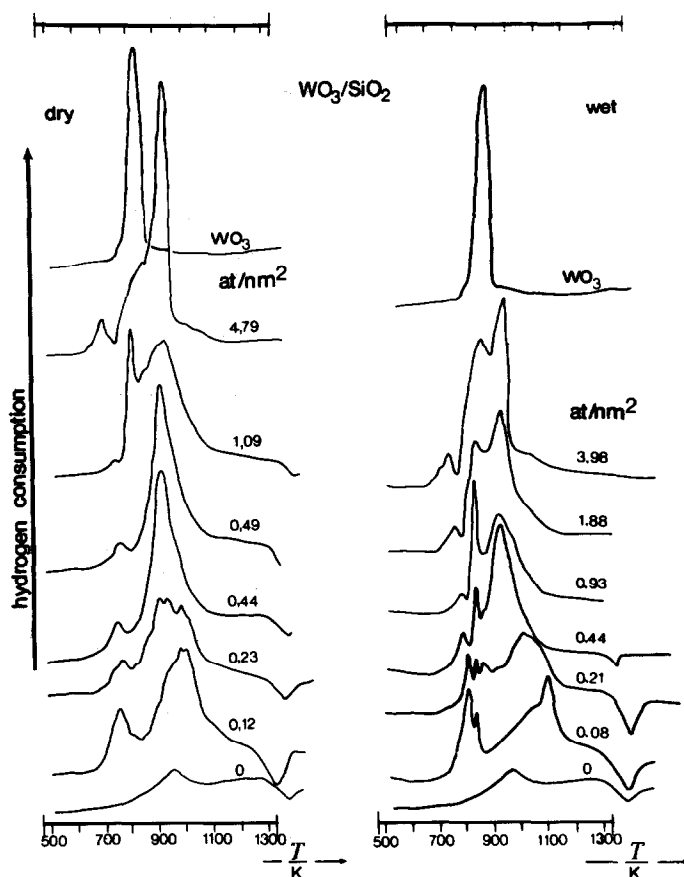


FIG. 2. TPR patterns of  $\text{SiO}_2$ ,  $\text{WO}_3$ , and  $\text{WO}_3/\text{SiO}_2$  catalysts prepared by dry and wet impregnation.

coverage of about 2 Mo atoms/ $\text{nm}^2$  and 5 W atoms/ $\text{nm}^2$  the silica-supported catalysts have a higher HDS activity than those supported on alumina.

#### Butene Hydrogenation Activity

The reaction rate constants  $k_2$  for the hydrogenation of butene are calculated as reported previously (1). The hydrogenation reaction is considered as a consecutive reaction, first order in butene. In Fig. 4 catalytic activity is characterized by  $k'_2$ , which is defined as the rate constant for hydrogenation,  $k_2$  ( $\text{m}^3$  butene converted) ( $\text{kg catalyst}^{-1} \text{s}^{-1}$ ), divided by the number of moles transition metal per kilogram catalyst. For both series of catalysts the impregnation method does not influence the hydrogenation

activity. Mo-based catalysts are slightly more active in hydrogenation at low surface coverages. At higher coverages, however, the two lines intersect. The hydrogenation activity vs surface coverage curves for the corresponding alumina-based catalysts (1) are also shown in Fig. 4.

$\text{MoO}_3/\text{SiO}_2$  has the same hydrogenation activity as  $\text{MoO}_3/\gamma\text{-Al}_2\text{O}_3$  up to approximately 1 Mo atom/ $\text{nm}^2$ ; at higher coverages the activity of  $\text{MoO}_3/\text{SiO}_2$  is much lower.  $\text{WO}_3/\text{SiO}_2$  is more active than  $\text{WO}_3/\gamma\text{-Al}_2\text{O}_3$  at surface coverages below approximately 2 W atoms/ $\text{nm}^2$ .

In Fig. 5 the ratio between hydrogenation and HDS rate constant is plotted as a function of surface coverage. W-based catalysts are relatively better hydrogenation cata-

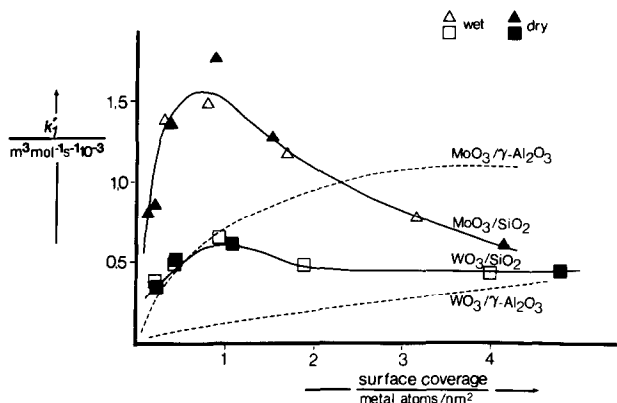


FIG. 3. Reaction rate constant  $k'_1$  for the hydrosulfurization of thiophene as a function of the average surface coverage for sulfided  $\text{MoO}_3/\text{SiO}_2$ ,  $\text{WO}_3/\text{SiO}_2$ ,  $\text{MoO}_3/\gamma\text{-Al}_2\text{O}_3$ , and  $\text{WO}_3/\gamma\text{-Al}_2\text{O}_3$  catalysts prepared by dry and wet impregnation (data for alumina-based catalysts are presented in Ref. (1)).

lysts than the corresponding Mo-based systems. Alumina-based catalysts hydrogenate relatively better than the corresponding silica-based catalysts.

## DISCUSSION

### Textural Properties

The observed differences in surface area and pore volume between the molybdenum

and tungsten catalysts may be due to pore blocking, as the pore radius distribution of the catalysts and the carrier are the same. The relatively strong decrease in surface area in the case of  $\text{MoO}_3/\text{SiO}_2$  is probably caused by pore blocking during calcination due to redistribution of active material via the vapor phase as  $\text{MoO}_2(\text{OH})_2$  (12).

The smaller decrease in pore volume for the catalysts with high transition metal con-

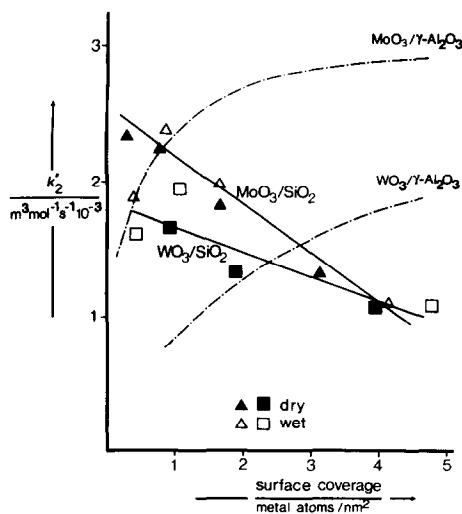


FIG. 4. Reaction rate constant  $k'_2$  for the hydrogenation of butene as a function of the average surface coverage for sulfided  $\text{MoO}_3/\text{SiO}_2$ ,  $\text{WO}_3/\text{SiO}_2$ ,  $\text{MoO}_3/\gamma\text{-Al}_2\text{O}_3$ , and  $\text{WO}_3/\gamma\text{-Al}_2\text{O}_3$  catalysts prepared by dry and wet impregnation (data for alumina-based catalysts are presented in Ref. (1)).

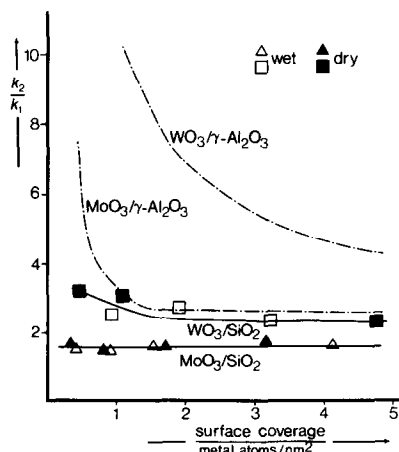


FIG. 5. Ratio between reaction rate constants from the hydrogenation of butene and the hydrosulfurization of thiophene,  $k_2/k_1$ , as a function of the average surface coverage, for sulfided  $\text{MoO}_3/\text{SiO}_2$ ,  $\text{WO}_3/\text{SiO}_2$ ,  $\text{MoO}_3/\gamma\text{-Al}_2\text{O}_3$ , and  $\text{WO}_3/\gamma\text{-Al}_2\text{O}_3$  catalysts, prepared by dry and wet impregnation (data for alumina-based catalysts are presented in Ref. (1)).



tent, compared with the decrease in surface area, is probably due to the method applied to determine the pore volume, viz. titration with water. It is reasonable to expect that at 295 K water can enter (partially) blocked pores easier than nitrogen at 77 K, e.g., by dissolving part of the transition metal compound layer or by diffusing through this layer. In accordance with this mechanism it is found that for these samples pore volumes obtained from the  $N_2$  desorption isotherm are smaller than those obtained by water titration.

#### *Temperature-Programmed Reduction*

**$MoO_3/SiO_2$ .** The broadness of the low-temperature peak at low Mo contents suggests a high dispersion, especially in the catalysts prepared by dry impregnation. For such monolayer-type catalysts often broad TPR peaks are observed, whereas bulk compounds in general show sharp TPR peaks. The explanation is that the carrier material usually exhibits heterogeneity, causing a spectrum of activation energies for reduction of compounds adsorbed on these sites, and as a consequence there is a broad TPR peak. Examples are alumina-supported molybdenum and tungsten oxide (1). When the interaction between carrier and active phase is low, the differences in activation energy will be less important and the peaks will be relatively sharp. An example is  $Re_2O_7/\gamma-Al_2O_3$  (14).

At higher Mo contents the sharpness increases, indicating a lower dispersion. The lower dispersion at higher Mo contents ultimately leads to the formation of crystalline  $MoO_3$  (XRD). In fact the presence of bulk  $MoO_3$  can also be concluded from the band at 900 K in the TPR patterns. From the relative area of this band the amount of crystalline  $MoO_3$  can be determined. It appears, however, that a discrepancy exists between the amounts of  $MoO_3$ , as derived from the area of the TPR band at 900 K, and the values obtained from XRD and XPS (Table 2). This problem was solved by means of a more detailed TPR study (4). From analysis

of the TPR pattern of  $MoO_3$  and a catalyst with high Mo content (21.4 wt%  $MoO_3$ ) at a low heating rate ( $1\text{ K min}^{-1}$ ) it was concluded that part of the low-temperature band is due to the reduction of crystalline  $MoO_3$ , probably to  $MoO_2$ .

**$WO_3/SiO_2$ .** On basis of the broadness of the reduction band, and analogously to the  $MoO_3/SiO_2$  system, it is concluded that at low W content the W compounds are slightly better dispersed when the dry impregnation technique is applied (Fig. 2). The sharp low-temperature bands in the patterns of the catalysts prepared by wet impregnation at low W contents are probably due to bulk compounds formed from dissolved carrier and tungsten ions, e.g., silicotungstic acid. At high W content crystalline  $WO_3$  is formed and the band at 800 K in these catalysts can be ascribed to reduction of crystalline  $WO_3$ . At the highest W contents again a discrepancy exists between the fraction of crystalline  $WO_3$  derived from TPR and the fraction derived from the combined results of XRD and XPS. Also here part of the high-temperature band apparently has to be assigned to the reduction of bulk  $WO_3$  (7).

On the average the reducibility of silica-based Mo(W) catalysts is better than that of alumina-based catalysts. This indicates that on silica a weaker interaction exists between the Mo(W) species and the carrier than on alumina.

#### *Thiophene Hydrodesulfurization*

Although the applied standard sulfiding procedure was shown to be satisfactory in the case of monolayer-type supported Mo catalysts (13, 15) it is to be expected that for those  $MoO_3(WO_3)/SiO_2$  catalysts which contain crystalline Mo(W) trioxide, sulfidation is not complete (13, 16). It is however improbable that for the  $MoO_3(WO_3)$  crystals of the present catalysts the extent of sulfiding is very critical. The surface of the active phase certainly will be sulfided (17) and as HDS catalysis will take place at the solid-gas interface it is probably not impor-

tant whether the interior of the crystals is sulfided or not.

The activity curve for  $\text{MoO}_3/\text{SiO}_2$  (Fig. 3) has a maximum at rather low surface coverage, which reflects the heterogeneity of the silica surface and its limited adsorption capacity. The position of the maximum coincides with the surface coverage at which crystalline  $\text{MoO}_3$  is formed in significant amounts. At this coverage the maximum amount of surface compounds is present (Table 2). Adding more molybdenum only results in the formation of crystalline  $\text{MoO}_3$ .

Sulfided bulk  $\text{MoO}_3$  has a low catalytic activity (Table 1). The (sulfided)  $\text{MoO}_3$  crystals on the catalysts apparently also have a low HDS activity per mole Mo, due to a poor dispersion and maybe also due to a low reducibility.

For  $\text{WO}_3/\text{SiO}_2$  the thiophene hydrodesulfurization activity curve again shows a maximum at a surface coverage of about 1 W atom/nm<sup>2</sup> and above this coverage the presence of  $\text{WO}_3$  crystals is observed in the XRD patterns. However, the activity decrease at higher surface coverages is less than in the case of  $\text{MoO}_3/\text{SiO}_2$  series. This difference can be due to differences in catalytic activity of the sulfided  $\text{MoO}_3(\text{WO}_3)$  crystals. As can be seen from Table 1, pre-sulfided unsupported  $\text{WO}_3$  is much more active in HDS than  $\text{MoO}_3$ . It should not be concluded, however, that this has a general validity, because it is likely that for these unsupported systems the activity is influenced by various factors, such as crystal size and crystal morphology.

$\text{MoO}_3/\text{SiO}_2$  is more active in HDS than  $\text{WO}_3/\text{SiO}_2$ . This has also been reported recently by Yermakov *et al.* (18, 19). The HDS activity per mole Mo(W) calculated for the alumina-based catalysts (Fig. 3) does not decline at high surface coverages. This is in agreement with the observation that no bulk compounds are formed in these systems. The curve for the  $\text{MoO}_3/\gamma\text{-Al}_2\text{O}_3$  systems levels off at a surface coverage of approximately 3 Mo atoms/nm<sup>2</sup>, while the

one for  $\text{WO}_3/\gamma\text{-Al}_2\text{O}_3$  increases continuously up to at least 5 W atoms/nm<sup>2</sup>. It has been suggested that this difference is due to a lower dispersion of the Mo species in comparison with the tungsten species, at higher surface coverage (4). The finding that the silica-based catalysts generally are more active than the alumina-based catalysts is in agreement with the results obtained by Yermakov *et al.* (18, 19).

#### Hydrogenation Activity

The relatively higher decrease in butene hydrogenation activity of  $\text{MoO}_3/\text{SiO}_2$  compared to  $\text{WO}_3/\text{SiO}_2$  (Fig. 4) can be understood from the fact that, under the test conditions applied, sulfided  $\text{WO}_3$  is more active in hydrogenation than sulfided  $\text{MoO}_3$  (Table 1).

The observation that the alumina-based catalysts are less active than the silica-based catalysts at low surface coverages can be explained by the higher reducibility of the silica-based catalysts. It is well known that low oxidation states are to be preferred in order to obtain high hydrogenation activity.

The fact that at higher transition metal contents alumina-based catalysts are more active than the silica-based ones can be explained by the presence of poorly dispersed crystalline  $\text{MoO}_3(\text{WO}_3)$  in the latter catalysts.

#### Relation between Hydrodesulfurization Activity and Reducibility

For the monolayer-type alumina-based catalysts it has been established that a correlation exists between reducibility (defined as the temperature at which under TPR conditions half the amount of hydrogen required for complete reduction of the  $\text{Mo}^{6+}(\text{W}^{6+})$  ions to  $\text{Mo}^0(\text{W}^0)$  was consumed) and HDS activity (1). This correlation is shown in Fig. 6.

Unlike the alumina-based catalysts the silica-based catalysts are not of the monolayer type over the whole range of transition metal content studied. In Fig. 6, there-

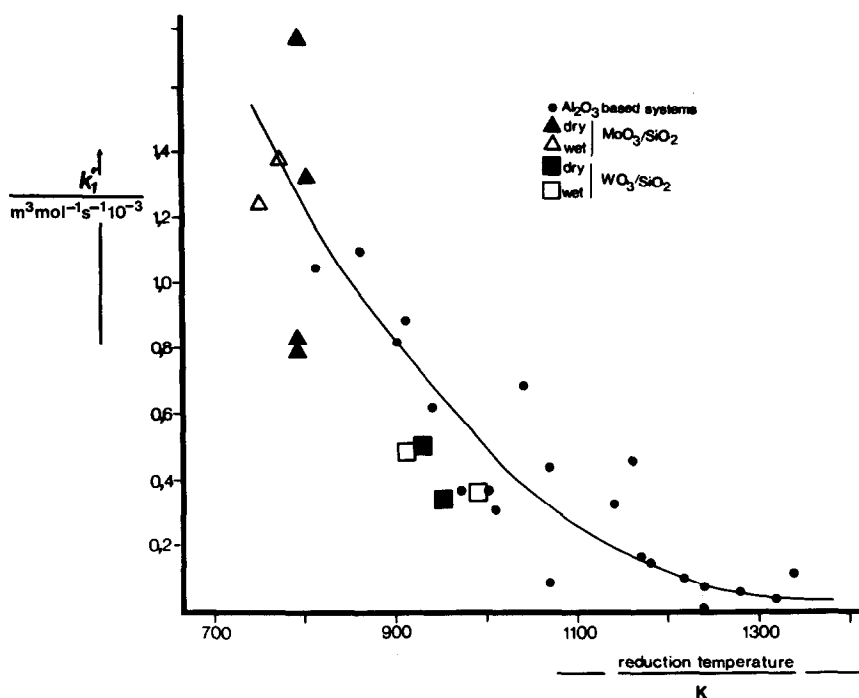


FIG. 6. Relation between the reaction rate constant  $k_1'$  for hydrodesulfurization of thiophene of sulfided  $\text{MoO}_3/\text{SiO}_2$ ,  $\text{WO}_3/\text{SiO}_2$ ,  $\text{MoO}_3/\gamma\text{-Al}_2\text{O}_3$ , and  $\text{WO}_3/\gamma\text{-Al}_2\text{O}_3$  catalysts and the average reduction temperature (data for alumina-based catalysts are presented in Ref. (1)).

fore, only the data of silica-based catalysts which do not contain crystalline material are plotted. Obviously for these catalysts the same relation between reducibility and HDS activity applies.

In principle it is also possible to take into account the other silica-based catalysts, containing crystalline material. To do so, corrections must be made for the amount of crystalline material present. This applies to HDS activity as well as reducibility of the remaining monolayer-type catalysts. As a consequence the value of  $k_1'$  will rise, and the reducibility will be higher for the  $\text{MoO}_3/\text{SiO}_2$  catalysts and lower for the  $\text{WO}_3/\text{SiO}_2$  catalysts.

The corrected HDS activities of the catalysts are plotted as function of the surface coverage in Fig. 7. It can be seen that the activity of  $\text{WO}_3/\text{SiO}_2$  monolayer catalysts increases with surface coverage, while the activity of  $\text{MoO}_3/\text{SiO}_2$  catalysts levels off at

surface coverages above approximately 0.5 Mo atom/nm<sup>2</sup>. It is striking that the shapes of these relations are similar to the relations found for  $\text{MoO}_3/\gamma\text{-Al}_2\text{O}_3$  and  $\text{WO}_3/\gamma\text{-Al}_2\text{O}_3$  catalysts (Fig. 3).

The present results and those previously obtained for analogous alumina-supported catalysts can be interpreted in a relatively simple way. The efficiency of the supported Mo(W) phase depends on two key properties of the oxidic precursor. The first concerns the dispersion, namely the higher the dispersion the higher the catalytic activity of the sulfided phase. The second concerns the sulfidation capacity; the easier sulfidation takes place, the higher the efficiency of the sulfided MO(W) phase. Apart from possible differences in the intrinsic activity of Mo and W complexes (1), the following interpretation emerges.

Alumina is a more reactive carrier than silica. Under the experimental conditions

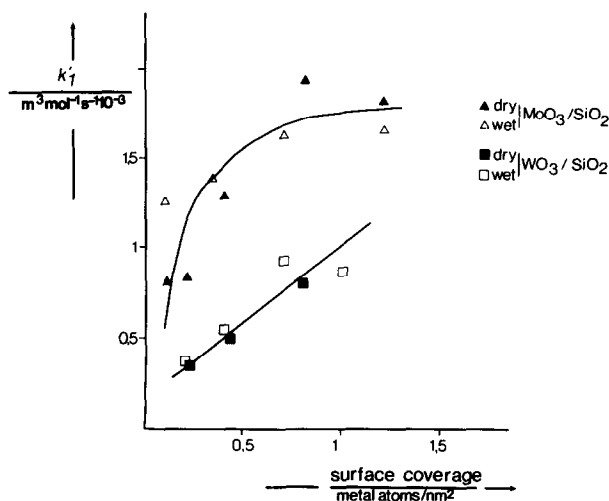


FIG. 7. Reaction rate constant  $k'_1$  for the hydrodesulfurization of thiophene as a function of the surface concentration, for sulfided  $\text{MoO}_3/\text{SiO}_2$  and  $\text{WO}_3/\text{SiO}_2$  catalysts, prepared by dry and wet impregnation.  $k'_1$  as well as the surface coverage have been corrected for the amount of crystalline  $\text{MoO}_3$  or  $\text{WO}_3$ .

applied in this study (type of carrier, pH, etc.) on alumina the maximum concentration of well-dispersed monolayer species is at least 5 transition metal atoms/ $\text{nm}^2$ , whereas on silica it is limited to ca. 1 transition metal atom/ $\text{nm}^2$ .

#### CONCLUSIONS

1. The impregnation method (wet or dry) does not influence the performance of  $\text{MoO}_3/\text{SiO}_2$  and  $\text{WO}_3/\text{SiO}_2$  catalysts.

2. At low metal oxide contents (calculated surface area below approximately 1 metal atom/ $\text{nm}^2$ ) the catalysts are of the monolayer type. At higher calculated surface coverages all extra Mo(W) added is present in the form of bulk compounds.

3. A correlation exists between the reducibility of the oxidic monolayer-type  $\text{MoO}_3/\text{SiO}_2$  and  $\text{WO}_3/\text{SiO}_2$  catalysts and the hydrodesulfurization activity of the corresponding sulfided systems. The higher the reducibility, the higher the catalytic activity. This correlation is the same as observed earlier for  $\text{MoO}_3/\gamma\text{-Al}_2\text{O}_3$  and  $\text{WO}_3/\gamma\text{-Al}_2\text{O}_3$  catalysts.

4. The butene hydrogenation activity of the sulfided  $\text{MoO}_3/\text{SiO}_2$  and  $\text{WO}_3/\text{SiO}_2$

monolayer-type catalysts also correlates with the reducibility of the corresponding oxidic systems.

#### ACKNOWLEDGMENTS

Thanks are due to M. C. Mittelmeijer-Hazeleger for TPR measurements, to A. Heeres for XPS measurements, to the Chemical Analysis Department of the Twente University of Technology, Enschede, The Netherlands, for XRF measurements, and to B. Koch and W. Molleman of the X-ray Spectrometry and Diffractometry Department, University of Amsterdam.

#### REFERENCES

1. Thomas, R., van Oers, E. M., de Beer, V. H. J., Medema, J., and Moulijn, J. A., *J. Catal.* **76**, 241 (1982).
2. Szekeley, J., Evans, J. W., and Solin, H. Y., "Gas-Solid Reactions." Academic Press, New York, 1976.
3. Klug, H. P., and Alexander, L. E., "X-Ray Diffraction Procedures." Wiley, New York, 1954.
4. Thomas, R., Ph.D. thesis, University of Amsterdam, 1981.
- 5., Houalla, M., and Delmon, B., *Surf. Interface Anal.* **3**, 103 (1981).
6. Kerkhof, F. P. J. M., and Moulijn, J. A. *J. Phys. Chem.* **83**, 1612 (1979).
7. Thomas, R., Moulijn, J. A., de Beer, V. H. J., and Medema, J., *J. Mol. Catal.* **8**, 161 (1980).

8. de Beer, V. H. J., van Sint Fiet, T. H. M., Engelen, J. F., van Haandel, A. C., Wolfs, M. W. J., Amberg, C. H., and Schuit, G. C. A., *J. Catal.* **27**, 357 (1972).
9. Kerkhof, F. P. J. M., Thomas, R., and Moulijn, J. A., *Recl. Trav. Chim. Pays-Bas* **96**, M121 (1977).
10. Castellan, A., Bart, J. C. J., Vaghi, A., and Giordano, N. *J. Catal.* **42**, 162 (1976).
11. Joint Committee on Powder Diffraction Standards Card 5-508.
12. Sonnemans, J., and Mars, P., *J. Catal.* **31**, 209 (1973).
13. de Beer, V. H. J., van der Aalst, M. J. M., Machiels, C. J., and Schuit, G. C. A. *J. Catal.* **43**, 78 (1976).
14. Yao, H. C., and Shelef, M., *J. Catal.* **44**, 392 (1976).
15. de Beer, V. H. J., Bevelander, C., van Sint Fiet, T. H. M., Werter, P. G. A. J., and Amberg, C. H., *J. Catal.* **43**, 68 (1976).
16. Grange, P., *Catal. Rev.—Sci. Eng.* **21**, 135 (1980).
17. Sanders, J. V., and Pratt, K. C., *J. Catal.* **67**, 331 (1981).
18. Yermakov, Yu. I., Startsev, A. N., Burmistrov, V. A., and Kuznetsov, B. N., *React. Kinet. Lett.* **14**, 155 (1980).
19. Yermakov, Yu. I., Kuznetsov, B. N., Startsev, A. N., Zhdan, P. A., Shepelin, A. P., Zaikovskii, V. I., Plyasova, L. M., and Burmistrov, V. A., *J. Mol. Catal.* **11**, 205 (1981).